

## RING EJECTION IN TYPE II SUPERNOVAE: 1E 0102.2–7219 IN THE SMALL MAGELLANIC CLOUD

IAN R. TUOHY AND MICHAEL A. DOPITA

Mount Stromlo and Siding Spring Observatories, Research School of Physical Sciences, Australian National University

Received 1982 July 2; accepted 1983 January 5

### ABSTRACT

We present a velocity map of the young oxygen-rich supernova remnant (1E 0102.2–7219) in the Small Magellanic Cloud, obtained with the Anglo-Australian Telescope. The velocity structure is complex and implies a high degree of asymmetry during the Type II supernova explosion. Our velocity data can be modeled in terms of a severely distorted ring of ejecta. This result, together with the evidence for expanding rings in similar remnants, suggests nonspherical ejection to be an intrinsic characteristic of Type II supernovae. We have also obtained two-dimensional spectroscopy of the diffuse halo of emission which partially surrounds 1E 0102.2–7219. The halo emits in the He II  $\lambda 4686$  line and is either a fossil H II region created by a UV flash accompanying the supernova, or alternatively, is being excited by intense UV radiation from the remnant itself. It is the first clear association of a high-excitation region with a supernova remnant.

*Subject headings:* galaxies: Magellanic Clouds — nebulae: supernova remnants — stars: supernovae — X-rays: sources

### I. INTRODUCTION

In a previous *Letter* (Dopita, Tuohy, and Mathewson 1981, hereafter Paper I), we reported the discovery of the optical counterpart of 1E 0102.2–7219, the brightest X-ray emitting supernova remnant (SNR) in the Small Magellanic Cloud (SMC) (Seward and Mitchell 1981). The optical remnant has a mean diameter of  $\sim 24''$  and consists of a series of filaments emitting predominantly in the forbidden lines of oxygen. A faint outer halo emitting in the lines of hydrogen and other elements partially surrounds the remnant. The annular region between the oxygen emitting filaments and the outer halo is almost devoid of emission, which we suggested in Paper I to be the result of ionization by the blast wave. This prediction is now supported by a high-resolution X-ray image of 1E 0102.2–7219, which shows that the total extent of the soft X-ray emission is  $\sim 40''$  (Tanaka 1982), comparable to the outer diameter of the dark annulus.

In this *Letter* we present the results of a detailed spectroscopic study of 1E 0102.2–7219 (a preliminary discussion has been given by Tuohy and Dopita 1982). Our two-dimensional spectra have allowed us to determine both the velocity structure of the expanding oxygen-rich ejecta and the nature of the surrounding halo of diffuse emission. The spectrophotometry of the ejecta will be discussed in a forthcoming publication (Dopita, Binette, and Tuohy 1983).

### II. OBSERVATIONS AND RESULTS

#### a) Velocity Structure

The observations of 1E 0102.2–7219 were made in 1981 June using the RGO spectrograph and the image photon counting system (IPCS) on the Anglo-Australian Telescope. A total of 11 long-slit spectra were taken with the slit aligned east-west, beginning just to the north of the [O III] emission (Paper I) and continuing south in steps of  $3''.0$ . The slit length was equivalent to  $2'.3$ , and the slit width was set to  $2''$  which was comparable to the seeing conditions at the time. Each spectrum, of  $\sim 1000$  s duration and  $\sim 8 \text{ \AA}$  resolution, comprised 2040 pixels spanning the wavelength range from  $3000 \text{ \AA}$  to  $7400 \text{ \AA}$ . For each of the 11 slit positions, a total of 58 spectra were recorded along the slit at a spacing of  $2''.3$ . A representative spectrum is depicted in Figure 1 (*upper*). The full-width velocity dispersion of the oxygen-rich material, determined from the complete set of spectra, is  $\sim 6500 \text{ km s}^{-1}$  ( $-2500$  to  $+4000 \text{ km s}^{-1}$ , relative to the local SMC standard of rest).

Narrow-band images have been constructed from the  $11 \times 58$  spatial grid of spectra, normalized for exposure time, by summing wavelength elements over velocity intervals centered on the [O II]  $\lambda 3727$  line (the [O III]  $\lambda 5007$  line was not used because of velocity overlap with the  $\lambda 4959$  component). The total [O II] emission from 1E 0102.2–7219 in the velocity range from  $-2500$  to

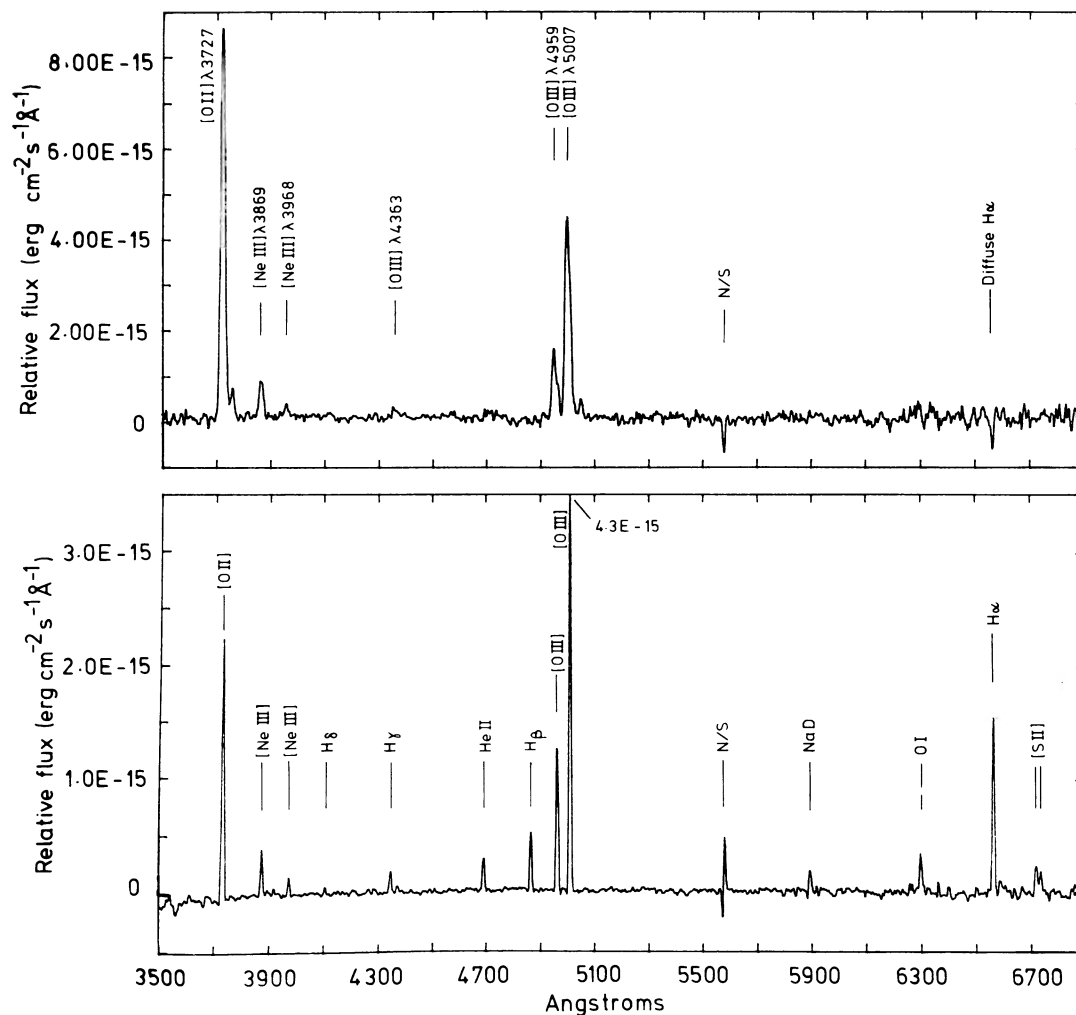


FIG. 1.—(upper) A representative sky-subtracted and calibrated spectrum of a filament in 1E 0102.2–7219. (lower) Spectrum of the diffuse halo which partially surrounds 1E 0102.2–7219. Note the He II  $\lambda 4686$  line.

+4000 km s<sup>-1</sup> is shown in Figure 2a (Plate L1). A continuum image (Fig. 2b) centered near 4000 Å has been subtracted from the [O II] image to provide approximate cancellation of the stellar component. For comparison purposes, we reproduce in Figure 3 (Plate L2) an enhanced version of the original [O III] image (Paper I) which has been partially deconvolved using a maximum entropy algorithm (Gull and Daniell 1978). Despite the restricted bandwidth of the [O III] image (960 km s<sup>-1</sup> FWHM), the appearance of the SNR agrees well with the lower resolution [O II] image (Fig. 2a) obtained by summing *all* high-velocity material.

In order to investigate the velocity structure of 1E 0102.2–7219, we have constructed a set of 12 narrow-band images, each equivalent to a velocity range of 520 km s<sup>-1</sup>. The 12 images are depicted as a mosaic in Figure 4 (Plate L3) and span the velocity range from -2600 km s<sup>-1</sup> to +3640 km s<sup>-1</sup>. It is clear from Figure

4 that the velocity structure of the SNR is both highly ordered and complex. In particular, the structure is not consistent with a simple expanding shell of material. The complexity is most apparent in the southeast quadrant of the SNR where a redshifted filament is seen to lie midway between two blueshifted filaments. All three filaments can be discerned more clearly in the high-resolution [O III] image (Fig. 3).

We have attempted to model the contorted velocity structure of 1E 0102.2–7219 in terms of an expanding ring of ejecta, in view of the evidence for ringlike structure in three other oxygen-rich SNRs (N132D: Lasker 1980; Cas A: Markert, Canizares, and Winkler 1981; and G292.0+1.8: Tuohy, Clark, and Burton 1982). For 1E 0102.2–7219, however, the ring cannot be coplanar. We can model the velocity structure by applying a  $\sin 3\theta$  modulation to a simple ring ( $\theta$  is measured in the plane of the ring) which produces oscillations in

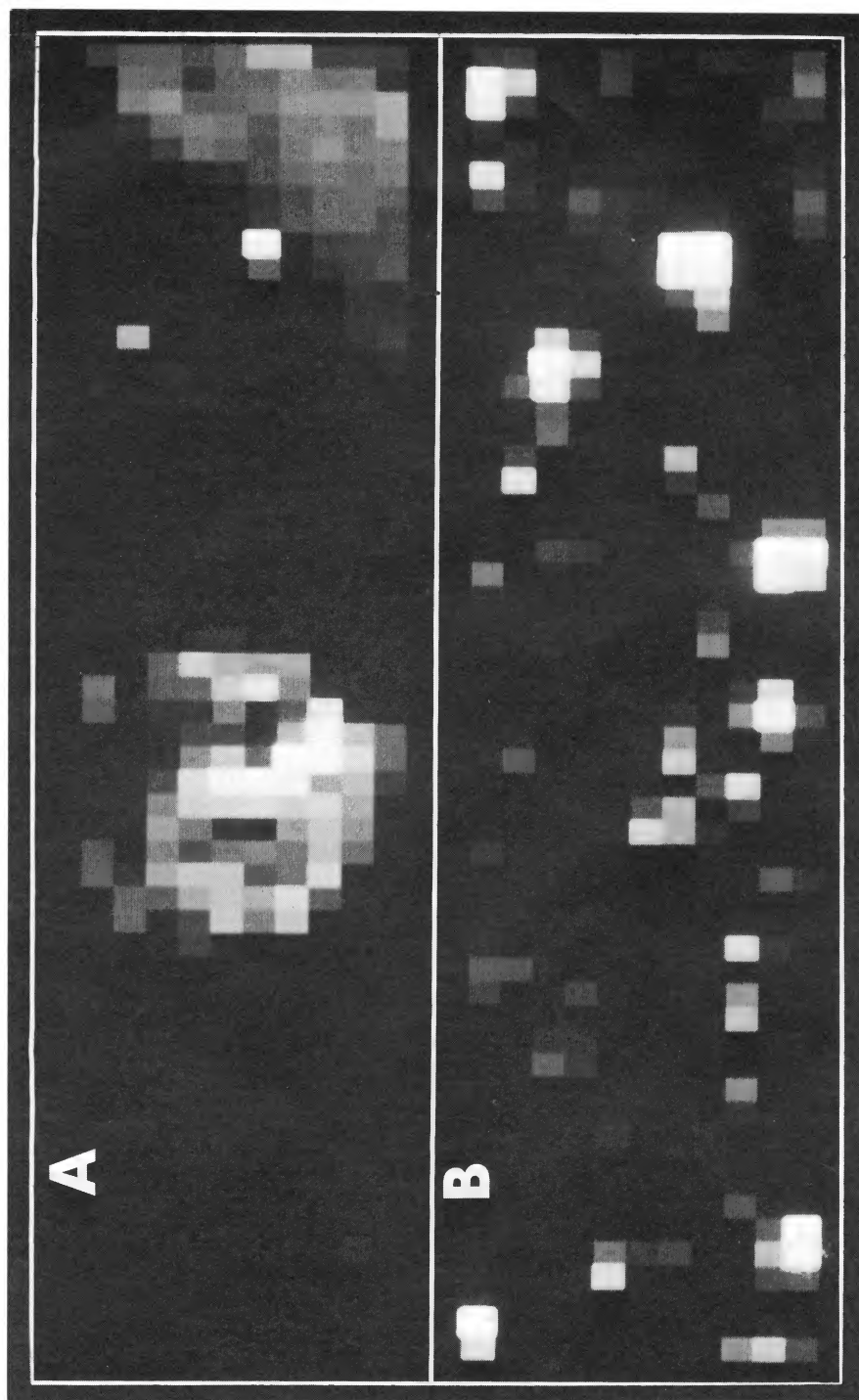


FIG. 2.—(a) An [O II] image of IE 0102.2–7219 (and N76 to the west) obtained by summing emission in the velocity range from  $-2500$  to  $+4000$   $\text{km s}^{-1}$ . A continuum image (Fig. 2b) has been subtracted to cancel the stellar component. Individual pixels measure  $3''0$  (N-S) and  $2''3$  (E-W). (b) A continuum image of the IE 0102.2–7219 field, centered near  $\lambda 4000$ .

TUOHY AND DOPITA (see page L12)

## PLATE L2

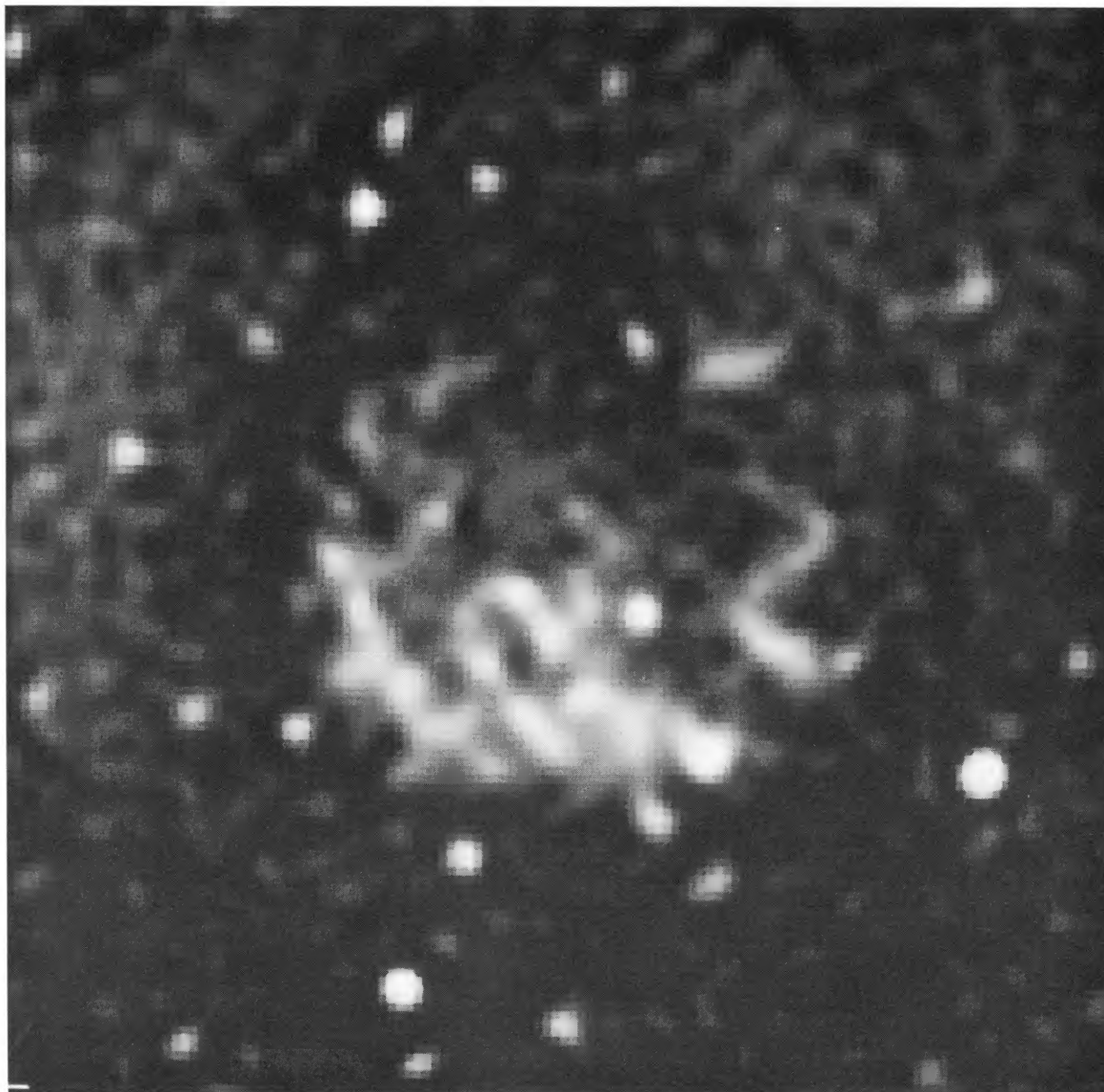


FIG. 3.—An enhanced version of the [O III] image of 1E 0102.2–7219 presented in Paper I (see text). The mean diameter of the filamentary region is  $\sim 24''$ .

TUOHY AND DOPITA (*see* page L12)

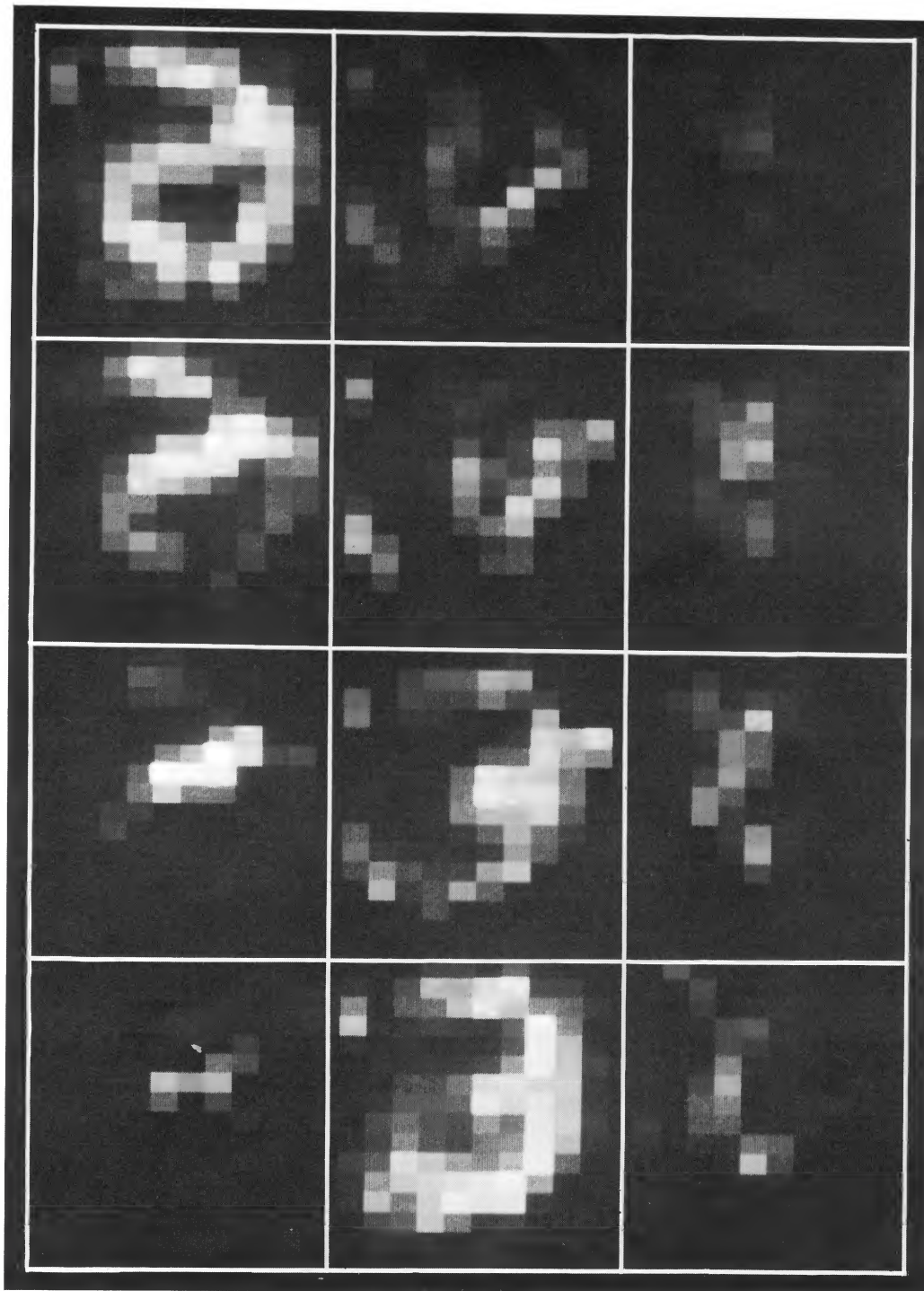


FIG. 4.—A mosaic of 12 images, showing relative intensities in velocity bands of  $520 \text{ km s}^{-1}$ . The sequence begins at  $-2600 \text{ km s}^{-1}$  (top left) and ends at  $+3640 \text{ km s}^{-1}$  (bottom right). The stellar component (Fig. 2*b*) has been subtracted. Pixel sizes match Fig. 2.  
TUOHY AND DOPITA (see page L12)

the orthogonal ( $\phi$ ) direction. An additional term is also needed to allow for an apparent variation in the amplitude ( $A$ ) of the oscillations as a function of  $\theta$ . Thus we adopt  $A(\phi) = A_0 [1 + \sin(\theta + \alpha)] \sin(3\theta + \beta)$ , where  $\alpha$  and  $\beta$  are phase shifts. The variables,  $A_0$ ,  $\alpha$ ,  $\beta$ , and inclination,  $i$ , of the polar axis of the twisted ring to the plane of the sky, were varied until a reasonable representation of both the spatial distribution of material and the velocity structure was obtained (the only significant feature in our data not represented by the model is a low-velocity filament in the northwest).

The twisted ring model, projected onto the plane of the sky, is depicted in a schematic three-dimensional representation in Figure 5. Values of  $A_0 = 30^\circ$ ,  $\alpha = -40^\circ$ ,  $\beta = 40^\circ$ , and  $i = 5^\circ$  have been used. While we emphasize that our model is idealized and approximate and that the uniqueness of the solution is not established, we find nevertheless that it gives an acceptable representation of the gross properties of the data. Better agreement could be obtained by reducing the symmetry inherent in our model. For example, the velocity may vary radially from the site of the explosion, and the oscillation period of the ring does not appear in our data to be constant at  $120^\circ$ , as implied by the  $\sin 3\theta$  term.

The age of 1E 0102.2–7219 can be estimated from our velocity data and the angular extent of the oxygen-rich filaments. Assuming constant velocity expansion and an SMC distance of 59 kpc (McNamara and Feltz 1980), we obtain an age of  $\sim 1000$  years. If the dark annulus surrounding the [O III] filaments does in fact

delineate the position of the shock front (§ I), our age estimate implies a mean shock velocity of  $\sim 4700$  km s $^{-1}$ .

### b) Surrounding Halo

Our two-dimensional spectroscopy of 1E 0102.2–7219 enabled spectra to be simultaneously obtained of the diffuse outer halo which partially surrounds the remnant. The extent of the halo is most clearly evident in Figure 6 (Plate L4) which shows the full  $\sim 3.5$  field of the original [O III] observation (Paper I). The halo emission is prominent due east of the SNR but is virtually absent in the inner annulus of sky immediately surrounding the [O III] filaments. We have therefore treated the annular area as background and produced a background-subtracted spectrum of the eastern halo region. The calibrated spectrum is shown in Figure 1(*lower*).

The halo spectrum has a Balmer decrement of  $H\alpha:H\beta = 2.9:1.0$ , which is typical of case B conditions and indicates that the reddening is low. The most unusual feature of the spectrum, however, is the presence of the high-excitation He II  $\lambda 4686$  line. It has a ratio relative to  $H\beta$  of 0.5:1.0 and a width of 8.7 Å FWHM which is consistent with the spectrograph resolution (i.e., any velocity broadening is less than 150 km s $^{-1}$ ). The [O III] intensity ratio,  $\lambda 4959 + 5007/\lambda 4363$ , of the halo is observed to be  $71 \pm 12$ . In view of the low reddening, this ratio indicates a temperature in the O $^{++}$  zone of

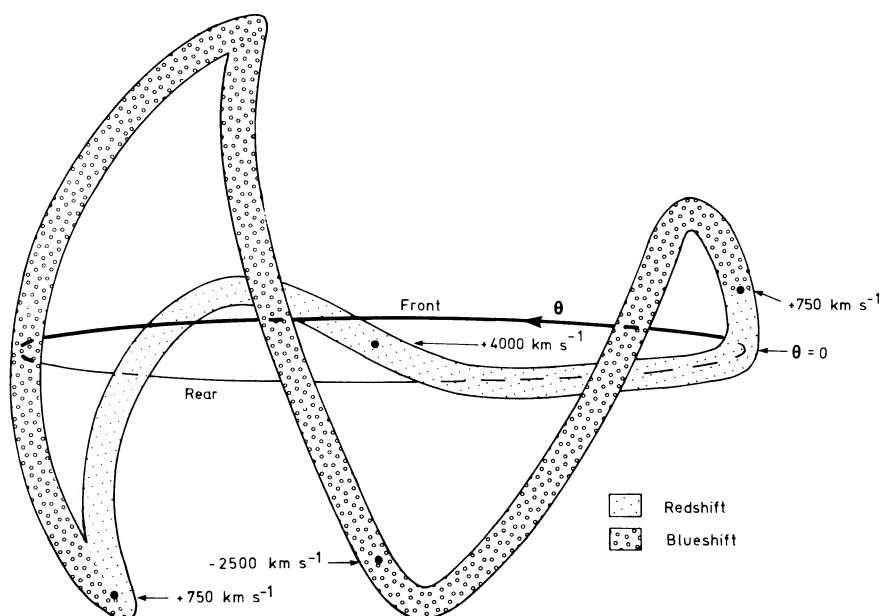


FIG. 5.—A schematic representation of the distorted ring model of 1E 0102.2–7219. Blueshifted and redshifted segments are indicated, together with model velocities based on a uniform expansion of 3250 km s $^{-1}$  from the center, superposed on a systemic velocity of +750 km s $^{-1}$ . The ellipse shows an undistorted ring, viewed from an angle of  $5^\circ$  below the plane of the ring.

## PLATE L4

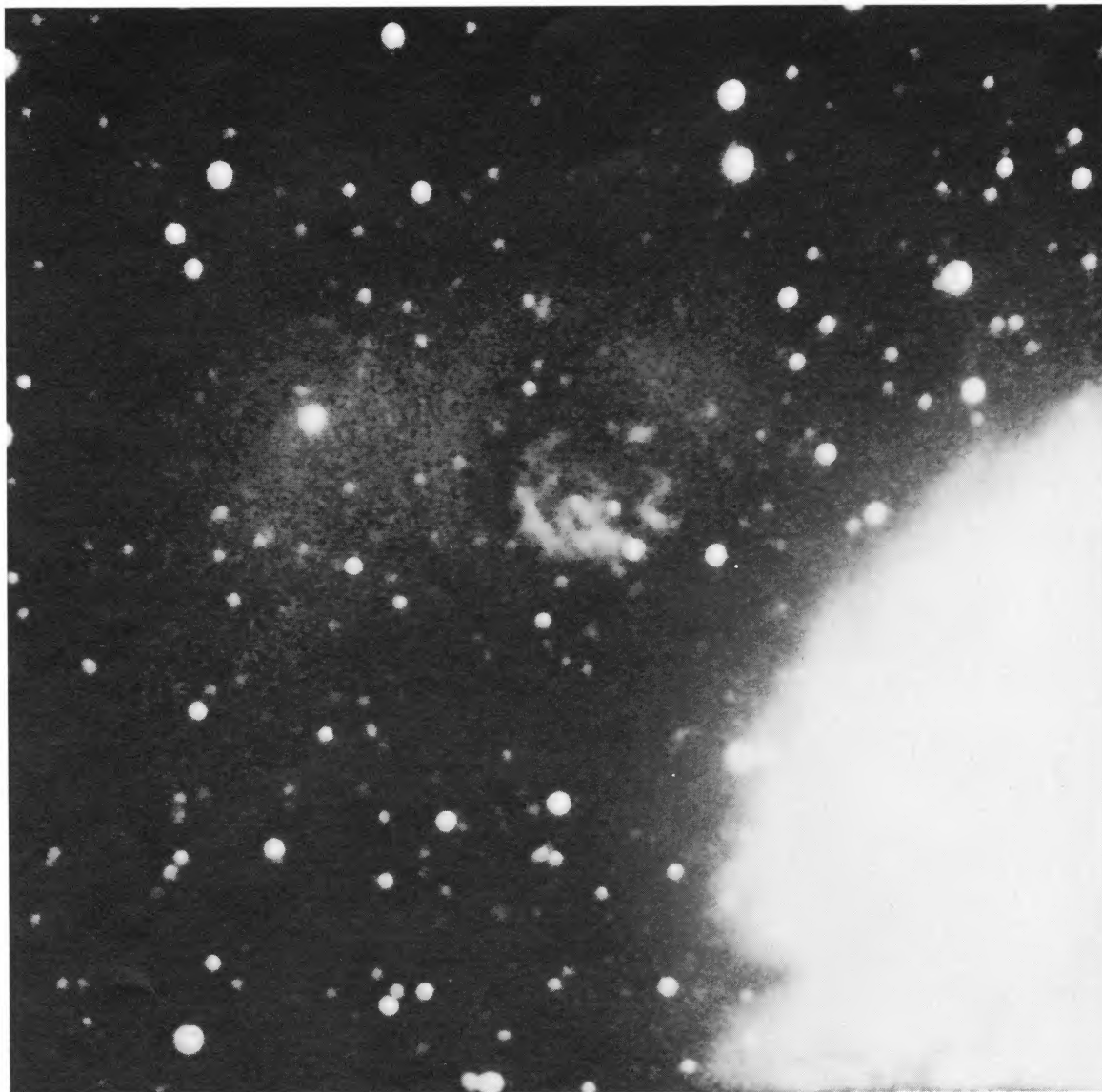


FIG. 6.—A full field ( $\sim 3.5'$ ) reproduction of the original [O III] observation of 1E 0102.2–7219 (Paper I), presented to show more clearly the extent of the diffuse halo emission.

TUOHY AND DOPITA (*see* page L13)

$15,300 \pm 1600$  K, similar or perhaps somewhat higher than other H II regions in the SMC. The  $\lambda 4686/\lambda 4861$  intensity ratio implies a  $\text{He}^{++}$  fractional abundance (by number with respect to hydrogen) of 0.05. Since He I recombination lines are not detected (the feature near  $\lambda 5890$  is improperly subtracted night-sky Na I D emission), we conclude that the halo shows no sign of a peculiar H/He abundance ratio that might be expected if it were the result of a presupernova stellar wind. This conclusion is in accord with the lack of velocity broadening.

### III. DISCUSSION

#### a) Dynamical Structure

The complex structure of 1E 0102.2–7219 provides compelling evidence for a high degree of asymmetry during the supernova explosion (assuming that the oxygen emission does in fact trace out the ejection pattern). The existence of expanding rings of ejecta has been inferred from the velocity structure of two other young SNRs containing high-velocity oxygen-rich ejecta, namely N132D (Lasker 1980) and Cas A (Markert *et al.* 1983). Furthermore, a recent high-resolution X-ray image of a third oxygen-rich SNR, G292.0+1.8, can also be interpreted in terms of an inclined ring of ejecta (Tuohy, Clark, and Burton 1982). The principal difference between 1E 0102.2–7219 and the foregoing three SNRs, however, is the evidence that the 1E 0102.2–7219 emission is not coplanar. In fact, our mathematical model suggests that the velocity vector sweeps between an angle of  $-30^\circ$  to  $+60^\circ$  relative to the plane of a simple undistorted ring. Some degree of perturbation from a coplanar ring cannot be discounted in N132D, Cas A, or G292.0+1.8. In this respect, the somewhat warped “X-ray bar” of G292.0+1.8 and the deviant outer pixels of N132D referred to by Lasker (1980) may be due to such an effect.

Bodenheimer and Woosley (1980, 1983) and Woosley and Weaver (1981*a, b*) have undertaken a two-dimensional study of a rotating  $25 M_\odot$  presupernova star whose core collapsed without generating a strong outgoing shock. This model formed a thick accretion disk in which explosive nuclear burning coupled with a rotational bounce near the core drove a high-velocity equatorial ejection of oxygen-rich material. Thus, such a model can explain the ejection of a planar ring. Gross oscillations orthogonal to the plane of the ring, however, would appear to require a further mechanism. It is possible that global instabilities are excited during the collapse phase, resulting in an initially warped accretion disk, but this would seem to require some kind of initial perturbation. A more promising potential explanation seems to lie in possible magnetized plasma instabilities in the explosion phase. If the magnetic field were purely radial during the initial collapse, the subsequent re-

expansion in the equatorial plane would form an expanding toroidal magnetic bubble, provided reconnection of lines of flux can occur. Thus, the conditions for development of the “fire-hose” instability (Parker 1958) may occur during the period of breakout of the oxygen-rich material from the star. This would result in an orthogonal component of velocity which would be amplified by the steeper polar density gradient.

#### b) Halo Emission Region

The clear association of a high-excitation halo emission region with 1E 0102.2–7219 is unique. The presence of a substantial abundance of  $\text{He}^{++}$  sets it apart from all other H II regions in galaxies—there is no case of a strong  $\lambda 4686$  line in any of these. On a spectral excitation classification, it is similar to a high-excitation planetary nebula. However, the high strength of some low-excitation lines such as [O II] and [S II] means that the halo emission region cannot be excited by a blackbody spectrum of sufficient temperature ( $T_* \approx 2 \times 10^5$  K) to ionize helium completely.

Since OB stars do not produce UV radiation of sufficient energy to account for the He II emission, there remain two possible explanations for the halo region. First, the halo could be a fossil H II region created by a UV flash at the instant of shock breakout through the photosphere of the star. Such regions have been predicted by theoretical considerations (e.g., Bottcher *et al.* 1970; McCray and Schwarz 1973). Second, it is possible that the halo is being excited by UV radiation from the SNR itself. The X-ray emission cannot be responsible, since it fails by several orders of magnitude to produce a sufficient specific intensity (the opacity of the surrounding gas to X-rays being very low). However, radiative shocks in the oxygen-rich material are much more prolific producers of UV emission. In particular, Itoh (1981*a, b*) has shown that radiative shocks faster than  $\sim 100 \text{ km s}^{-1}$  produce an extensive precursor, which could account for the observed ionization.

### IV. CONCLUDING REMARKS

The number of SNRs known with certainty to have been produced by Type II supernovae on the basis of their oxygen-rich spectra has increased from one (Cas A) to a total of six in recent years. In addition to 1E 0102.2–7219, the new members of the class are G292.0+1.8 (Goss *et al.* 1979; Murdin and Clark 1979), N132D (Lasker 1978, 1980), 0540–69.3 (Mathewson *et al.* 1980), and an unresolved SNR in NGC 4449 (Balick and Heckman 1978; Kirshner and Blair 1980). Two common characteristics of this group of “Type II SNRs” are becoming apparent. These are:

1. The oxygen-rich ejecta have a structure suggesting preferential expulsion in the equatorial plane. There is now evidence for this in four of the Type II SNRs

(N132D: Lasker 1980; Cas A: Markert *et al.* 1983; G292.0+1.8: Tuohy, Clark, and Burton 1982; and 1E 0102.2–7219). Neither of the remaining two remnants have been velocity mapped, partially because of their small angular sizes. Ring ejection and the evidence for severe distortion of the ring in at least one SNR should therefore be taken into account in detailed modeling of Type II supernovae.

2. Most, if not all, Type II SNRs are associated with faint H II regions centered on the remnants (van den Bergh 1971; Balick and Heckman 1978; Murdin and

Clark 1979; Lasker 1980). While some of these may be photoexcited by OB stars, this *Letter* provides clear evidence that at least one is directly related to the supernova event (or remnant).

We thank Professor Don Mathewson for helpful discussions, and Dr. Y. Tanaka for communicating the results of his X-ray observations prior to publication. We are also indebted to the staff of the Anglo-Australian Observatory for their excellent support of this project.

## REFERENCES

- Balick, B., and Heckman, T. 1978, *Ap. J. (Letters)*, **226**, L7.  
 Bodenheimer, P. B., and Woosley, S. E. 1980, *Bull. AAS*, **12**, 833.  
 ———. 1983, *Ap. J.*, submitted.  
 Bottcher, C., McCray, R. A., Jura, M., and Dalgarno, A. 1970, *Ap. Letters*, **6**, 237.  
 Dopita, M. A., Binette, L., and Tuohy, I. R. 1983, in preparation.  
 Dopita, M. A., Tuohy, I. R., and Mathewson, D. S. 1981, *Ap. J. (Letters)*, **248**, L105 (Paper I).  
 Goss, W. M., Shaver, P. A., Zealey, W. J., Murdin, P., and Clark, D. H. 1979, *M.N.R.A.S.*, **188**, 357.  
 Gull, S. F., and Daniell, G. J., 1978, *Nature*, **272**, 686.  
 Itoh, H. 1981a, *Pub. Astr. Soc. Japan*, **33**, 1.  
 ———. 1981b, *Pub. Astr. Soc. Japan*, **33**, 521.  
 Kirshner, R. P., and Blair, W. P. 1980, *Ap. J.*, **236**, 135.  
 Lasker, B. M. 1978, *Ap. J.*, **223**, 109.  
 ———. 1980, *Ap. J.*, **237**, 765.  
 Markert, T. H., Canizares, C. R., Clark, G. W., and Winkler, P. F. 1983, *Ap. J.*, **268**, in press.  
 Mathewson, D. S., Dopita, M. A., Tuohy, I. R., and Ford, V. L. 1980, *Ap. J. (Letters)*, **242**, L73.  
 McCray, R., and Schwarz, J. 1973, *The Gum Nebula and Related Problems*, ed. S. P. Maran, J. C. Brandt, and T. P. Stecher (NASA SP-332; Washington, D.C.: GPO).  
 McNamara, D. H., and Feltz, K. A. 1980, *Pub. A.S.P.*, **92**, 587.  
 Murdin, P., and Clark, D. H. 1979, *M.N.R.A.S.*, **189**, 501.  
 Parker, E.N. 1958, *Phys. Rev.*, **109**, 1874.  
 Seward, F. D., and Mitchell, M. 1981, *Ap. J.*, **243**, 736.  
 Tanaka, Y. 1982, private communication  
 Tuohy, I. R., Clark, D. H., and Burton, W. M. 1982, *Ap. J. (Letters)*, **260**, L65.  
 Tuohy, I. R., and Dopita, M. A. 1982, Paper presented at *IAU Symposium 101, Supernova Remnants and their X-Ray Emission*, Venice, Italy, 1982 August–September.  
 van den Bergh, S. 1971, *Ap. J.*, **165**, 259.  
 Woosley, S. E., and Weaver, T. A. 1981a, *Ann. NY Acad. Sci.*, **375**, 357.  
 ———. 1981b, Proc. NATO Advanced Study Institute on Supernovae, Ed. D. Arnett, J. Lattimer, R. Stoneham and M. Rees, Cambridge, England, June–July 1981.

M. A. DOPITA and I. R. TUOHY: Mount Stromlo and Siding Spring Observatories, Private Bag, Woden P.O., A.C.T. 2606, Australia